# Microgrid Protection Using Low-Cost Communication Systems

Jerome Nsengiyaremye, *Student member*, *IEEE*, Pal C. Bikash, *Fellow*, *IEEE*, and Miroslav M. Begovic, *Fellow*, *IEEE*

***Abstract*—Power electronics interface of renewable energy to system is now the trend in both transmission and distribution segments of power network. Unlike synchronous generators the fault feeding, and control characteristic of these renewable generators are different and mostly influenced by the topology, switching, control deployed in power electronics interface. So, the network protection design and operational requirements are now challenged in the absence of large fault current. Although the differential current principle still works, its implementation is limited by the significant cost associated to its communication system. This paper proposes a differential line protection scheme based on local fault detection and comparing binary state outputs of relays at both ends of the line thus requiring a simple, flexible and low bandwidth communication system. The performance of the proposed scheme is assessed through simulation of an example system with several scenarios.**

***Index Terms*—Distributed generation (DGs), Fault-ride through, Inverter interfaced distributed energy resource (IIDER), Inverter-only microgrid.**

## I. Introduction

With the availability of cost effective solar and wind energy conversion technologies, power electronics driven microgrid for electrifying remote areas is now the preferred option. It is also an option for more reliable energy solution in the contexts of large cities. The energy and transport infrastructures of many modern cities are planned as a single system from energy point of view. Power electronics being an interface between renewable energy sources and network, the fault current flow behavior in the network is very dominated by its control.

Microgrid is not a brand new concept though. It dates back to the beginning of power system industry in the end of 19$^{th}$ century. However, it is only in the past two decades that it attracted significant research interest because the technology of generation has changed, influencing operational characteristics and requirements of the system. One important such requirement is protection against fault. In many cases, there is a departure from traditional radial topology of feeders, which totally changes the type of protection that is possible to use. Traditionally, due to high cost of expanding the national grid to remote rural areas, microgrids have been assumed to be reasonably an economic alternative, and operate as isolated small grids. However, it has become necessary to meet energy requirements of cities from its generation from roof-top solar etc. with guaranteed reliability when the national grid fails. With higher levels of quality of power supply and reliability demanded by consumers over time, some distribution feeder automation strategies such as reclosers, sectionalizers, whose purpose may be related to protection have been adopted as practical solutions. This paper, however, focuses on addressing the major issue of change of type of protection instead of tackling the entire problem together.

From strategic operational perspective, it is required to plan, design and operate microgrid in a flexible way. Flexibility is realized when microgrid is able to operate in grid-connected as well as in islanded mode. Power electronics offers the flexibility but influences the fault behavior of the system, which renders the standard network protections less effective. Inverter interfaced distributed energy resources (IIDERs) in grid distribution systems compromise conventional distribution system protection schemes such as overcurrent protection which is widely used in traditional radial feeders in the absence of local distributed generation [1], [2]. The ineffectiveness of such schemes becomes more pronounced in IIDER-based microgrids operating in islanded mode. This is because local generators can easily deviate from grid operation requirements such as voltage and frequency nominal values [3]. A flexible microgrid requires a robust protection strategy. Recent research has dealt with these challenges and new protection schemes have been proposed, and extensively discussed [4].

Despite much research effort in microgrid protection, practically transmission-based protection schemes are used due to lack of appropriate microgrid protection design standards and relays [5]. Unfortunately, in distribution microgrids, most of the schemes such as distance and overcurrent directional relays become ineffective as well [1], [5]. For example, due to line lengths that may not be sufficiently long to provide zoned protection, distance relays are likely to fail. Furthermore, in systems dominated by IIDERs, the predefined fault current references make the fault current phase angles completely independent of prefault voltage, which also challenges the performance of distance relays [5]. Due to the complexity of inverter fault current limiting function, especially when multiple inverters are feeding into a fault via meshed microgrid, thus creating potentially overlapping ranges of operating and fault currents, the performance of conventional overcurrent directional relays is affected. Typically, the overcurrent feature of these relays is adversely affected by low fault currents generated by IIDERs as they are restricted to a maximum value close to the rated current to protect the inverter components while the directionality feature is affected by the independent characteristic of current phase angle with respect to the voltage [5]. Furthermore, inverters being typically ungrounded, and most of inverters only generating positive sequence currents even during unbalanced fault conditions, the directionality feature that is not based on positive sequence currents may

not be reliable for the protection of microgrids dominated by IIDERs [1], [5].

Differential protection principle typically meets the technical requirements to protect microgrids due to its immunity to the non-sensitivity to bidirectional power flow, changing current levels, number of distributed energy resources (DERs) in the microgrid, microgrid operation mode and weak infeed [4], [6], [7]. However, it has been demonstrated that much attention should be taken in choosing the differential parameter as traditional differential current relay may become ineffective in some situations when the IIDER penetration is high [8], [9]. This is due to the effect of the difference between the sequence components of the fault currents on both sides of the line [8] as the system becomes mainly influenced by inverter control.

Research studies recently undertaken based on data mining approach have identified appropriate parameters for microgrid protection [8], [10], [11]. It has been shown that positive and negative sequence current components are among top three features for both fault detection and localisation [11], [12]. Of these two features, the positive sequence current components are preferable due to their presence in all types of faults [8], [10], [13]–[16].

While it is technically effective, the current differential protection requires the exchange of the measurements from both ends of the line, which requires high bandwidth, sophisticated and significantly expensive communication systems. The cost of such communication systems may hinder the adoption of conventional differential protection in distribution systems and microgrids, whose level of investment is relatively low. However, it has been shown that the schemes with no communication link between relays cannot effectively protect microgrids from all types of faults [6], [17]. So a protection scheme that allows the use of a low-cost communication system is considered viable, and perhaps the only alternative.

One way of reducing the communication cost requirement is to minimize the size of the information to be exchanged between the relays without jeopardizing the accuracy of the fault detection and faulted line localization. So with minimal information size, a low bandwidth communication system can be used as its cost is relatively low.

This paper proposes such a line protection scheme using positive sequence currents estimated at both ends of the line. These currents are assessed to extract the current directionality information in the form of binary states. This information is obtained using a novel simple and straightforward technique that detects the change in the current flow direction at each end of the line. Contrary to differential conventional protection, the exchange of information between the line relays does not require data synchronisation.

As most communication-assisted protection schemes in the literature do not comprehensively cover the communication aspect by routinely assuming the availability of systems that meet the protection requirements, this paper provides a case study of a low-cost communication system that can be used with the proposed protection scheme in distribution systems. Section II presents the IIDERs behaviour under fault conditions. The protection scheme principle details are discussed in Section III while Sections IV and V assess and discuss the performance of the proposed protection scheme under various scenarios. Section VI concludes the paper.

## II. IIDER BEHAVIOUR UNDER FAULT

### A. Plant description

Full-scale power converters are becoming indispensable in network integration of wind turbine and solar power. The configuration of the inverters adopted in this study is a three-phase three-wire topology usually used in medium voltage distribution systems [18]. Each inverter is connected to the rest of the microgrid through an LCL filter. The filter is formed of an LC circuit and a step-up transformer. The microgrid side of the LC circuit is considered as the point of the common coupling (PCC) at which the IIDER is connected to the rest of the microgrid. It is at the PCC that the voltage and current are measured for control and protection of the inverter. This is illustrated by the black background side of Fig. 1. It could be possible to consider measurements taken after the transformer, but high voltage level would challenge the cost-effectiveness of voltage measurement. For the simplicity of the control system, the generator is assumed to produce a (DC) voltage.

### B. Inverter behavior under faults

The behavior of inverters under fault in microgrid is determined by the injected current at the PCC. This current depends on the inverter control system. Moreover, to protect electronic components of the inverter from damage, its fault current is limited to a maximum value close to the rated current. The limiting strategy of the current is practically achieved by providing preset current references to the current controller when the voltage loop controllers generated references exceed a set threshold. The general structure of the IIDERs control is given by the white background of Fig. 1. The signals generated by the VSC under different fault types measured at the filter inductor outputs and at the PCC are displayed in Fig. 2.

With the fault ride through conditions, the smart inverter will generate reactive power to the system during faults. So contrary to synchronous generators in transmission systems where the fault currents depend on the impedance of the passive elements of the network, the angle of the fault current in IIDERs will mainly depend on the control system. However, this does not mean that the traditional angular features used for protection in transmission systems can be straightforwardly used in synchronous machine-based microgrids because of the challenges posed by short lines.

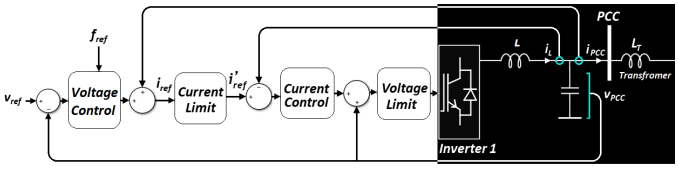


Fig. 1. Voltage source control

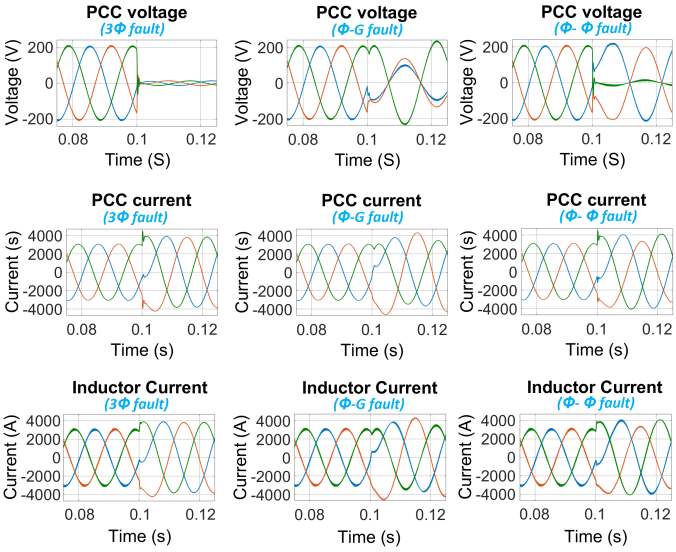


Fig. 2. Voltage and current signals measured at PCC and at the output of the filter inductor in different fault conditions (three phase fault (3Φ), single phase to ground fault (Φ-G), and phase to phase fault (Φ-Φ))

As multi-DER microgrids contain at least two DGs, power sharing strategy should be considered during fault with respect to the system stability. It has been shown that among the most used techniques, droop-based and master-slave, the droop-based approach is more robust [19]. Consequently, due to its sensitivity to fault, the master-slave technique is ideal for testing the effectiveness of any protection scheme.

## III. Protection Scheme

### A. Fault detection

For the simplicity of fault detection analysis, a robust and reliable microgrid system shown in Fig. 3 is used. Typically, when a fault occurs at Point F on Line $L_{BE}$ one of the line relays, 3 or 4 will see a change in current flow direction with respect to the prefault current flow direction. So the change in current direction can be a useful indication of a fault on the line. It is important to note that this is true when the line considered does not present any taps. The fault detection under this study does not cover tapped lines, which are commonly not used in network like microgrids under consideration. Otherwise, an extension to the proposed scheme is possible and should be sought.

Conventionally, current flow direction estimation has been based on the comparison of the voltage and current phase angles. However, with no voltage measurement devices installed at every node in distribution systems, current-only based techniques become necessary. Schemes based on current-only approach proposed in the literature, so far, are only for fault direction estimation [13], [14], [20]–[23]. Research in [13], [20], [21] compares prefault and fault current phase angles to determine if a fault is upstream or downstream of the relay. However, this is limited to radial systems where prefault power flow direction is known, and a separate fault detection device is required. On the other hand [14] applies directly the phase

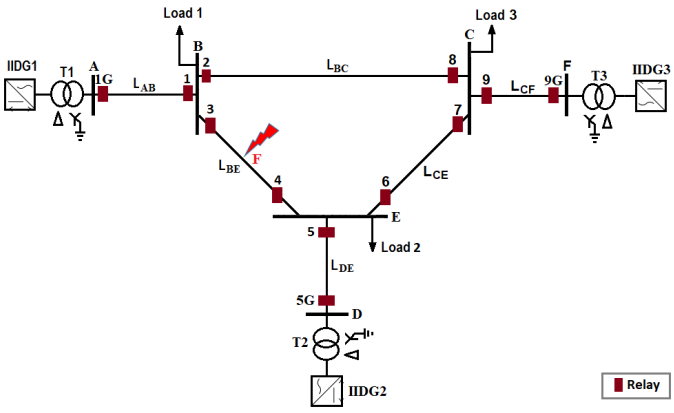


Fig. 3. Study microgrid system

comparison approach which requires the exchange of the phase angle values between relays. In [22], [23], the fault direction is estimated at both end of the line to detect an internal fault. For the approach in [22], the relay at each end of the line detects a fault on a fraction of the line based on an overcurrent principle. This scheme is only effective in grid connected microgrids with the grid providing significantly higher fault current than the DGs.

The study in [23] proposes an interesting approach based on fault direction estimation technique proposed in [13], [20], [21] by considering the fault direction estimation at both ends of the line. This study, however, has analysed and verified this approach with extra high voltage transmission system data which may not necessarily be consistent with distribution systems.

While the difference between the local prefault and fault current phase angles could be used, as in [23], a clever, yet simple approach to detecting a change in current flow direction keeping the prefault angle as the reference is to calculate the cosine of the angle. When there is a change in direction, the cosine value changes the sign. This approach offers a new simple comparison reference, “zero”, as a constant and neutral number. In three-phase systems, the positive sequence current is used. Therefore, for simplicity, the word “current” is subsequently adopted in this study to refer to positive sequence current.

*The proposed approach can be equivalent to the principle of phase comparison protection scheme with the difference that, in this paper, the compared quantities are measured at one end of the line at two successive instants and then compare the transition patterns (events) from both ends rather than directly comparing the two quantities measured at the two ends of the line at the same instant. Moreover, the proposed principle is built on full cycle Fourier technique recognised for its inherent immunity to harmonics.*

The proposed protection scheme uses “the zero” as the reference for detection of the change in current flow direction by computing the cosine value of the current phase angle. The relay fault detection principle and the phasor computation

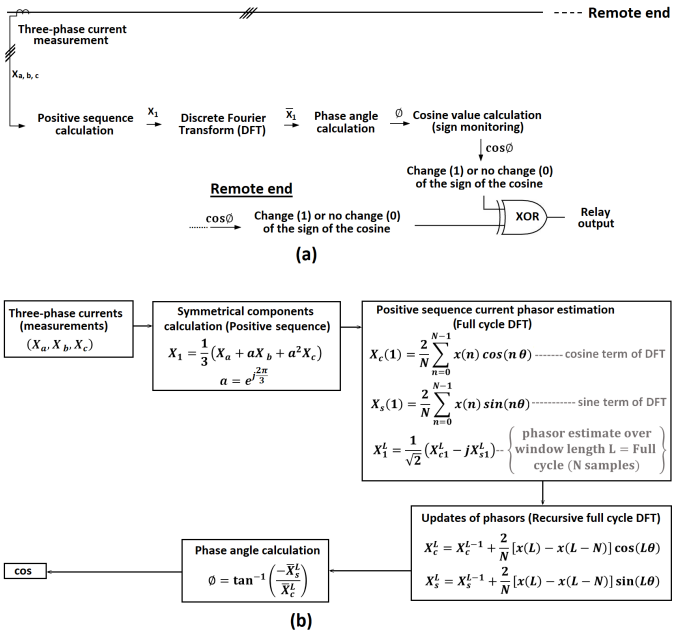


Fig. 4. Fault detection strategy: (a) principle (b) phasor estimation

algorithm are provided in Fig. 4. The phasor estimation is based on full cycle discrete Fourier transform (DFT) due to its deterministic aspect and capability to reject harmonics. Non-Fourier algorithms such as least squares-based algorithms, differential-equations algorithms, Kalman filter algorithms and Walsh functions algorithms suffer from harmonic effect and might not attain the required online speed computation [20], [24]. The update of phasor estimates with time are computed using recursive full cycle technique. This technique offers computational simplicity and provides a stationary phase angle in steady state by default as one of the side benefits.

When a fault occurs on a line, one of the ends of the line experiences a change in current flow direction (i.e. the change of its cosine value sign) while the other does not get affected much. With each line-end relay capturing the current direction transition, the fault on the line is detected by the relays by exchanging their current direction information. When both relays register the same direction transition (no change or a change in current direction) there is no fault detected on that line. On the contrary, if one of the relays registers a change, a fault is detected on the line.

It may happen that there is no current flowing in the line before fault occurrence. In this case, the relay is not able to take a decision on the change of current direction. To tackle this issue, two assumptions are made:

- When the current is zero or very small, its phase angle is set to zero i.e. the cosine is "one".
- While it may not necessarily be the case when the current is flowing in a line prior to fault occurrence, the monitoring directions of relays at both ends of the line must be the same. This means that the current transformers supplying measurements to the relays must be consistently polarized, and both relays consistently installed. This convention allows the definition of the same virtual reference (cos (0) = 1) for the cosine value sign for both relays. Therefore, the relay can virtually decide a change of current direction or a no-change condition.

The latter assumption above does not only solve the direction change issue but also allows correct discrimination of fault from load switching events. Under load switching events, both relays register the same transition pattern (no change or change of current direction), which is also the case for an external fault.

As previously mentioned, the exchange of information between the line relays requires a communication channel. Since the adoption of communication-assisted protection schemes may be hindered by the cost of the communication system, the current direction transitions (the change or no change) are directly transformed into binary states, "1" or "0" in order to allow the use of simple and low-cost communication systems. Moreover, this offers flexibility in data transmission.

### *B. Low-cost communication system*

The overall cost of a communication system comprises the cost of the communication equipment (physical link and interfaces), the installation cost (work and labor), the required installation time, and its reliability. The cost comparison analysis of existing communication systems has shown that unlicensed microwave radio offers practically the lowest cost option [25]. Its low cost is due to the nonrequirement of right of way, low installation cost, low cost of labor (no specialized expertise), and short installation time [25]–[28]. The two most used spread-spectrum techniques for unlicensed radio communication are frequency hopping spread spectrum (FHSS) and direct-sequence spread spectrum (DSSS). Both techniques can be used for protection applications. The FHSS offers more reliability at low frequency band, typically 902-928 MHz [24].

To ensure low-cost communication system feasibility, the protection scheme should offer flexibility in reducing the message size. On the other hand, the presence of other functions, for example the control signals for master-slave power sharing strategy, which rely on communications may relieve some of the pressure in that respect.

### *C. Practical considerations of low-cost communication system with the proposed protection scheme*

To analyze the communication requirements, the proposed protection scheme is classified as a teleprotection scheme. Standard practice requires a certain level of reliability of such schemes to adhere to. The standard sets the security as the probability of unwanted command to be between $10^{-4}$ and $10^{-8}$, and the dependability as the probability of missing command to be between $10^{-2}$ and $10^{-4}$ [27]. This means that one unwanted trip requires a minimum of $10^{8}$ noise bursts for a scheme designed with $10^{-8}$ security [29].

The proposed protection scheme is evaluated for the most stringent requirements among teleprotection schemes i.e. $10^{-8}$ security. To achieve such a level of security, it is important to ensure that if a distinct message was corrupted, it should not be received as a valid message. It is therefore necessary not to send binary 1 and 0 as they are, because a corrupted binary 1 might become a binary 0 and vice-versa. To tackle this issue, two approaches are usually used i.e. redundant bits, and duplicate messages [29]. However, the former increases the bandwidth requirement affecting the dependability as expressed in (1) while the latter approach may require extra memory that might increase the cost and time delay for the fault detection.

$$P_{mc} = 2k(BER) \tag{1}$$

where $P_{mc}$ is the probability of missing command, $k$ the number of bits in a message, and $BER$, the bit error rate defined as the ratio of erroneous bits to total bits transmitted on a digital channel.

Fortunately, the proposed protection scheme, being phasor-based, has an inherent typical delay of one cycle (20 ms for 50 Hz nominal frequency). Despite not usually desirable, this delay can allow the relay to send the same message more than once in a cycle without a memory, thus creating a natural duplicate message approach. Furthermore, it is a standard practice that a protection message is sent two to eight times per cycle [26], [27]. A combination of this natural duplicate message and the bit redundancy approaches offers an opportunity to achieve the required security and dependability with a low bandwidth channel requirement and short transmission time. The total time delay associated with radio communication system can then be evaluated based on the message size, the number of messages exchanged per cycle, the relay processing time, the channel bandwidth capacity, and the allowed communication channel latency [29].

While radios are characterized by high latency, technologies with variable latency are recommended for teleprotection. These types allow for setting changes of some features that require much processing time with no value addition to the scheme application [27]. Such features are forward error correction (up to 5 ms), message acknowledgement, retry or re-transmission, data buffering ($\sim$ 50 ms), and encryption ($\sim$ 10 ms) [27]. This is because the relay sends data continuously allowing the receiving relay to get the right message even when some are corrupted. Practically radio latency of 2 ms is achieved [29]. Currently, unlicensed radios exist with bandwidth as high as 38400 bps that can achieve the range of 15 to 30 km [26].

To evaluate the feasibility of the whole scheme (fault detection and communication), a simple serial digital to digital bit stream communication protocol is considered. This protocol can use interfaces such as Universal Asynchronous Receiver Transmitter (UART) or Ethernet for message transmission [29], [30]. Taking the UART interface as an example, the message size to be exchanged between relays can be assessed. This interface can allow 1 to 23 bits per data word in addition to an overhead of two bits (typically one start bit and one stop bit) (message) [31]. This gives flexibility in choosing the appropriate word size for some applications. For many applications, the most common data word size is 8 bits. Along with this message size, two others are compared in Table I in terms of their associated delays: 25-bit, and 16-bit messages.

To obtain the total time required by the proposed scheme to output a decision, the relay delay ($\sim$ 20 ms), and the transmission interface delay ($\sim$2 ms, typically between 1-5 ms) are added to the total communication time delay. This time is about 41.3 ms, 36.4 ms, and 36.7 ms for the 10-bit, 16-bit, and 23-bit message sizes respectively. So, the scheme requires about 2 cycles. This is typically acceptable for protection applications as it is well below the critical clearing time requirement for microgrids reported in the literature (about 5 cycles) [19], [32]. This assessment has assumed a full duplex communication channel. However, a half-duplex system can be used by automatically switching the channel in both direction [29]. This would farther reduce the communication system cost but at the expense of response time. This would add a delay of about a cycle bringing the total response time to about 3 cycles. This time should also be acceptable because circuit breakers can clear the fault in less than 2 cycles.

It is important however, to highlight that the proposed protection scheme may not be appropriate for special systems requiring very high speed protection. Current differential protection can be used, otherwise an extension to the proposed scheme based on fractional data window may be sought.

Also, for any communication-assisted protection scheme, the failure of communication system leaves the system unprotected. It is therefore important to have a back-up protection protection in place to ensure the system protection in a such situation.

## IV. Study System

A medium voltage microgrid system, with loop configuration, is used as a study system as shown in Fig. 3. While there are no impediments to using the same or similar technique applied to a more traditional, radial grid with many laterals, the extensive presence of tapped extensions and use of automation would require more in-depth analysis. Nevertheless, this is a reasonable configuration to first try the concept as it represents a reliable isolated grid, and a reasonably challenging case to evaluate the effectiveness of the proposed protection scheme.

TABLE I
Comparison of communication system delays of different message sizes

| | **10 bits** | **16 bits** | **25 bits** |
|---|---|---|---|
| Transmission time (ms) | 0.26 | 0.42 | 0.65 |
| Allowed latency (ms) | 2 | 2 | 2 |
| Receiving Interface delay (ms) | 2 | 2 | 2 |
| Relay reporting rate delay (ms) | 15 | 10 | 10 |
| **Total communication delay (ms** | **19.26** | **14.42** | **14.65** |

### A. Positive sequence equivalent circuit

The positive sequence equivalent circuit of the study system with a three-phase fault on Line $L_{BE}$ is given in Fig. 5. The inverter interfaced distributed generator (IIDG) is represented by the positive sequence current source [14], [15], [33].

When a three-phase fault occurs on line $L_{BE}$, the positive sequence fault current $I_F$ is given by the sum of faults currents $L_{BF}$ and $L_{EF}$ from buses B and E respectively as expressed in (2).

$$I_F = I_{BF} + I_{EF} \tag{2}$$

$$I_{BF} = I_{F\_IIDG1} + I_{F\_IIDG3\_CB}$$

and

$$I_{EF} = I_{F\_IIDG2} + I_{F\_IIDG3\_CE}$$

where $I_{F\_IIDG1}$ and $I_{F\_IIDG2}$ are positive sequence fault currents generated by IIDG1, IIDG2 while $I_{F\_IIDG3\_CB}$ and $I_{F\_IIDG3\_CE}$ are positive sequence fault current flowing respectively through branches $CBF$ and $CEF$ from IIDG3.

The fault currents passing through the two branches are function of the branch impedances and IIDGs currents as expressed in (3) and (4).

$$I_{F\_IIDG3\_CB} = \frac{I_{F\_IIDG3}(Z_{CE} + Z_{EF})}{(Z_{CB} + Z_{BF}) + (Z_{CE} + Z_{EF})} \tag{3}$$

$$I_{F\_IIDG3\_CE} = \frac{I_{F\_IIDG3}(Z_{CB} + Z_{BF})}{(Z_{CB} + Z_{BF}) + (Z_{CE} + Z_{EF})} \tag{4}$$

where $Z_{CE}$, $Z_{EF}$, $Z_{CB}$, $Z_{BF}$, $Z_{CE}$, and $Z_{EF}$ represent line impedance of Lines $L_{CE}$, $L_{EF}$, $L_{CB}$, $L_{BF}$, $L_{CE}$, and $L_{EF}$ respectively.

Recognising that the parameter characteristics of the lines forming the loop are typically almost the same, since each line should handle the same maximum current when one of the line is isolated, and that the lines in the microgrid are short (the same length assumption would make sense for a loop configuration in this case), the fault current $I_F$ could be estimated as follows

$$I_F = \left(I_{F\_IIDG1} + \frac{I_{F\_IIDG3}}{2}\right) + \left(I_{F\_IIDG2} + \frac{I_{F\_IIDG3}}{2}\right) \tag{5}$$

The positive sequence current values generated by the inverter for each type of fault are provided by the manufacturer as required by the standard [33]. Typically, the fault current value is limited to a maximum value close to the rated inverter current. IIDGs with low voltage fault ride-through capability are required to generate reactive current to support the system voltage stability during fault [5]. This to equivalently say that these IIDGS generate low power factor power during faults. With inverters usually controlled in $dq0$ reference frame, the power factor can be estimated using the ratio of quadratic component $i_q$ to the direct current component $i_d$.

From (5) it can be observed that positive sequence fault current angles depend mainly on the IIDGs fault currents i.e. their power factor. This offers simplicity in developing line protection schemes for inverter-only microgrids. This is because it becomes possible to do the analysis with an assumption of two current sources, one at each end of a line with prior knowledge of the current phase angle value range.

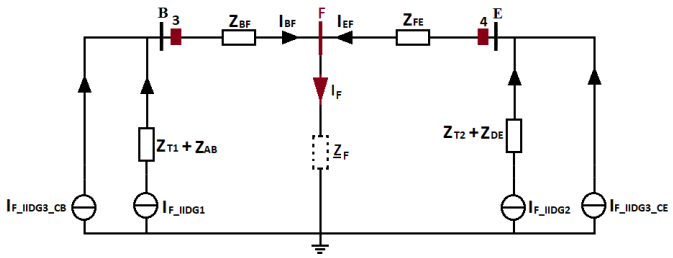


Fig. 5. Positive sequence equivalent circuit with a fault on Line $L_{BE}$

## V. Simulation Scenarios and Results

### A. Simulation scenarios

To validate the effectiveness of the proposed scheme, a microgrid study model was developed in Matlab/Simulink environment. The topology of the model given in Fig. 3 is

TABLE II
STUDY MICROGRID PARAMETERS

| **IIDER Parameters** | | | |
|---|---|---|---|
| | **IIDG1** | **IIDG2** | **IIDG3** |
| Rated power (kW) | 1000 | 1000 | 1000 |
| Rated voltage (V) | 260 | 260 | 260 |
| DC bus voltage (V) | 500 | 500 | 500 |
| Fundamental frequency (Hz) | 50 | 50 | 50 |
| Switching frequency (kHz) | 5 | 5 | 5 |
| Filter inductance (mH) | 0.04 | 0.04 | 0.04 |
| Filter resistance (mΩ) | 0.067 | 0.067 | 0.067 |
| Filter capacitance (mF) | 1.2 | 1.2 | 1.2 |
| Damping resistance (mΩ) | 28 | 28 | 28 |
| Current control proportional | 0.248 | 0.248 | 0.248 |
| Current control integral | 0.42 | 0.42 | 0.42 |
| Voltage control proportional | 0.748 | 0.748 | 0.748 |
| Voltage control integral | 0.00 | 0.00 | 0.00 |
| **Step-up Transformer Parameters** | | | |
| Rated power (kVA) | 1200 | 1200 | 1200 |
| Rated primary voltage (kV) | 0.260 | 0.260 | 0.260 |
| Rated secondary voltage (kV) | 20 | 20 | 20 |
| Winding configuration | D1Yg | D1Yg | D1Yg |
| Fundamental frequency (Hz) | 50 | 50 | 50 |
| Winding inductance (pu) | 0.03 | 0.03 | 0.03 |
| Winding resistance (pu) | 0.001 | 0.001 | 0.001 |
| **Line Parameters** | | | |
| Line type | Overhead | | |
| Positive sequence parameters | Resistance (Ω/km) | Reactance (Ω/km) | Susceptance ($\mu$S/km) |
| | 0.510 | 0.366 | 3.172 |
| Zero sequence parameters | Resistance (Ω/km) | Reactance (Ω/km) | Susceptance ($\mu$S/km) |
| | 0.658 | 1.611 | 1.280 |

The length of the lines in km: $L_{AB} = L_{CF} = L_{ED} = 0.6$, $L_{BC} = 3.0$, $L_{BE} = 1.5$, and $L_{CE} = 1.0$.

used. The parameters of the IIDGs, step-up transformers, and power lines are provided in Table II. The IIDG1 adopts the Voltage-Frequency control to form and maintain the voltage and frequency of the system at reference values while the others are locally controlled as current sources. To ensure appropriate power sharing among IIDGs, the master-slave control is adopted. The IIDG1 operates as the master, and shares its current reference signals to other IIDGs (the slaves). This strategy is chosen due to its simplicity and highest sensitivity to faults. The control process is performed in synchronous reference frame (dq0). To limit the fault current generated by IIDGs and overvoltage under unbalanced faults, the latched current limiting strategy, and the instantaneous saturation limit are respectively adopted.

Three scenarios namely Reference Scenario, Scenario 1, and Scenario 2 are assessed under this study.

*a) Reference scenario:* This scenario assesses the effectiveness of the protection scheme versus fault type, fault resistance, and fault location. The existence of prefault currents in all branches of the microgrid loop is assumed and ensured by the following load conditions: Load 1 = 0.7 MW; Load 2 = 1.3 MW and Load 3 = 0.2 MW. The fault currents are limited to 1.2 times the value of the rated inverter current, an ideal value to challenge the proposed scheme and even more to conventional scheme. The power factor is set to 0.56 (lagging) i.e. $i'_{dref} = 0.67\ pu$ and $i'_{qref} = -1.0\ pu$. These predefined fault current references are assumed to be the same for all three IIDGs. Different types of faults i.e. symmetrical (L-L-L-G) and unsymmetrical faults (L-G and L-L) were simulated on Line $L_{BE}$ (between relays 3 and 4) and Line $L_{AB}$ (between Relays 1G and 1) at time instant $t = 0.1\ s$.

*b) Scenario 1:* This scenario evaluates the effectiveness of the proposed protection scheme for different fault inception time instants, and for different reactive current values generated by IIDGs during fault. With the former, a fault on Line $L_{BE}$ at two fault inception instants different from the Reference Scenarios are considered; $t = 0.11\ s$, and $t = 0.116\ s$. On the other hand, different power factors (PF) are considered in the following three cases:

- The fault current references for all IIDGs are limited to 1.2 pu with a power factor of 0.85 (lagging) i.e. $i'_{dref} = 1.02\ pu$ and $i'_{qref} = -0.63\ pu$.
- The fault current references for all IIDGs are limited to 1.2 pu with a power factor of 0.2 (lagging)i.e. $i'_{dref} = 0.24\ pu$ and $i'_{qref} = -1.17\ pu$.
- The fault current references for all IIDGs are limited to 1.2 pu with different power factors. The power factor of IIDG1 (PF 1) = 0.85; PF 2 = 0.56, and PF 3 = 0.2.

Other than the fault inception time instants, and fault current references, the parameters and conditions under Scenario 1 are the same as in the Reference Scenario.

*c) Scenario 2:* This scenario assesses the performance of the proposed protection scheme in case of load switching. This scenario has been undertaken considering two cases:

- the performance of the scheme when there is current flowing in a line prior to fault occurrence; and
- the performance of the scheme when there is no current flowing through at least one of the loop lines prior to fault occurrence.

Since the fault events are comprehensively covered in the previous scenarios when there is current flowing in the lines prior to fault, the first case under this scenario will only consider load switching event. The initial loading under this case is such that Load 1 = 0.5 MW, Load 2 = 0.8 MW, and Load 3 = 0.2 MW. At t = 0.1 s a an additional load of 0.5 MW is switched on at Bus B.

The second case on the other hand, considers both load switching and fault events. This is because it is a special case not covered in the previous scenarios. Initially, all loads at the nodes are set to 0.5 MW. With such loading, there is no current flowing in the loop as the IIDGs can satisfy their respective local loads. To assess the performance of the scheme, at t = 0.1 s a three phase fault is simulated on Line $L_{BE}$. For the load switching events, with the same loading condition, an additional load of 0.6 MW is connected at Bus B at t = 0.1 s. With this additional load kept in the system, the 0.6 MW are switched off from the system at t = 0.15 s in order to verify the effectiveness of the scheme when a considerable load is switched off from the system.

Other than the loading parameters, other simulation parameters are the same as those of the Reference scenario.

### B. Simulation results

The cosine values computed by each relay over time for a three-phase solid fault are provided in Fig.6. It is clearly that only Relay 4 registers a change in the cosine value sign just after the fault inception time. With the rest of relays registering a no-change direction state, the fault is detected between Relays 3 and 4 as it is the only relay pair to register different cosine sign transitions. This case is reflected in Fig. 7 illustrating the current flow direction in the study system before and during the fault (note that due to line styles used to demarcate the cosine values computed by different relays in the figure, some values seem to be greater than one while they are actually not). A full picture of the simulation results is

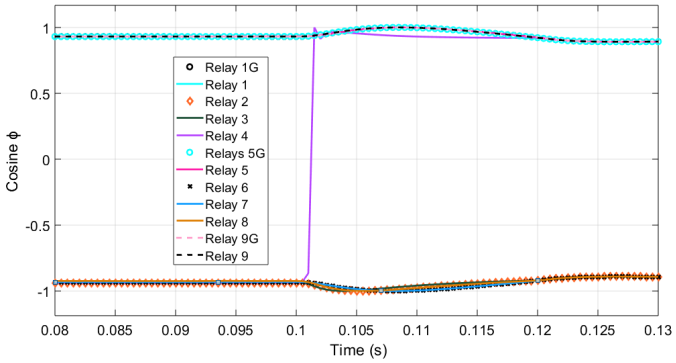


Fig. 6. The cosine values computed by relays for a three-phase fault on Line $L_{BE}$

TABLE III
PERFORMANCE OF THE PROPOSED PROTECTION SCHEME

| Event type | | 1G | 1 | 2 | 8 | 3 | 4 | 5 | 5G | 6 | 7 | 9 | 9G |
|---|---|---|---|---|---|---|---|---|---|---|---|---|---|
| **Positive sequence current phase angle (degree)** | | | | | | | | | | | | | |
| **Prefault** | | 21.3 | 21.3 | -160.1 | -157.7 | -158.5 | -159.4 | 21.2 | 21.3 | -159 | -158.9 | 21.3 | 21.3 |
| **Cosine value sign** | | + | + | - | - | - | - | + | + | - | - | + | + |
| **Fault on Line $L_{BE}$ (between Relays 3 and 4)** | | | | | | | | | | | | | |
| $R_f = 0\ \Omega$ | L-L-L-G | -26.8 | -26.8 | 153.2 | 153.2 | 153.1 | -26.8 | -26.8 | -26.8 | 153.2 | -153.2 | -26.8 | -26.8 |
| | L-G | -26.4 | -26.4 | 153.8 | 154.3 | 154.2 | -25.4 | -26.3 | -26.3 | 153.6 | 153.6 | -26.3 | -26.3 |
| | L-L | -26.4 | -26.4 | 153.7 | 154.2 | 154.1 | -25.5 | -26.4 | -26.4 | 153.5 | 153.5 | -26.4 | -26.4 |
| $R_f = 100\ \Omega$ | L-L-L-G | -28.3 | -28.3 | 151.5 | 151.9 | 151.7 | -28.3 | -28.3 | -28.3 | 151.6 | 151.7 | -28.2 | -28.2 |
| | L-G | 17.2 | 17.1 | -167.4 | -166.3 | -170.4 | 1.6 | 17.2 | 17.2 | -163.3 | -163.2 | 17.1 | 17.2 |
| | L-L | -3.2 | -3.2 | 173.6 | 174.5 | 171.9 | -11.8 | -3.2 | -3.2 | 176.4 | 176.5 | -3.2 | -3.2 |
| $t = 0.110\ s$ | L-L-L-G | -26.8 | -26.8 | 153.2 | 153.2 | 153.1 | -26.8 | -26.8 | -26.8 | 153.2 | -153.2 | -26.8 | -26.8 |
| | L-G | -26.4 | -26.4 | 153.8 | 154.3 | 154.2 | -25.4 | -26.3 | -26.3 | 153.6 | 153.6 | -26.3 | -26.3 |
| $t = 0.116\ s$ | L-L-L-G | -26.8 | -26.8 | 153.2 | 153.2 | 153.1 | -26.8 | -26.8 | -26.8 | 153.2 | -153.2 | -26.8 | -26.8 |
| | L-G | -26.4 | -26.4 | 153.8 | 154.3 | 154.2 | -25.4 | -26.3 | -26.3 | 153.6 | 153.6 | -26.3 | -26.3 |
| PF = 0.85 | L-L-L-G | -2.4 | -2.4 | 177.5 | 177.5 | 177.5 | -2.5 | -2.4 | -2.4 | 177.6 | 177.6 | -2.4 | -2.4 |
| | L-G | -3.4 | -3.4 | 177.5 | 178 | 178.4 | -0.8 | -3.4 | -3.4 | 176.6 | 176.7 | -3.4 | -3.3 |
| PF = 0.20 | L-L-L-G | -49.1 | -49.1 | 130.9 | 130.9 | 130.8 | -49.1 | -49 | -49 | 130.8 | 130.9 | -49.1 | -49.1 |
| | L-G | -43.4 | -43.8 | 133.7 | 134.1 | 132.6 | -49.2 | -43.5 | -43.5 | 136.2 | 136.3 | -43.4 | -43.4 |
| Different PFs | L-L-L-G | -2.5 | -2.5 | 125.2 | 125.2 | 163.4 | -34.1 | -26.8 | -26.8 | 134.3 | 134.3 | -49.1 | -49.1 |
| | L-G | -2.9 | -2.9 | 112.6 | 112.9 | 171.4 | -39.2 | -27.8 | -27.8 | 131.6 | 131.6 | -51.8 | -51.8 |
| **Cosine value sign** | | + | + | - | - | - | + | + | + | - | - | + | + |
| **Change in cosine value sign** | | No | No | No | No | No | Yes | No | No | No | No | No | No |
| **Fault discrimination from load switching event** | | | | | | | | | | | | | |
| Prefault for Case 1 (initial loading) | | 22.6 | 22.5 | -159.6 | -155.8 | -157.2 | -159.2 | 22.5 | 22.6 | -158 | -157.7 | 22.5 | 22.6 |
| Load connection | | 21.48 | 21.4 | -159.2 | -158.2 | 21.1 | 21.5 | 21.4 | 21.4 | -158.8 | -158.6 | 21.5 | 21.5 |
| Prefault for Case 2 (initial loading) | | 22.5 | 22.5 | 0 | 0 | 0 | 0 | 22.4 | 22.5 | 0 | 0 | 22.5 | 22.5 |
| Load connection | | 21.6 | 21.6 | -159.5 | -158 | 21.1 | 21.5 | 21.5 | 21.5 | -159.8 | -158.5 | 21.5 | 21.5 |
| Load disconnection (after load connection) | | 22.5 | 22.5 | 0 | 0 | 0 | 0 | 22.4 | 22.5 | 0 | 0 | 22.5 | 22.5 |
| Fault | | -2.5 | -2.5 | 177.5 | 177.5 | 177.5 | -2.5 | -2.5 | -2.5 | 177.5 | 177.5 | -2.5 | -2.5 |

- $R_f$, PF and t refer to fault resistance, power factor of fault reference currents of IIDGs, and fault inception time respectively.
- Different PFs refers to PF 1 = 0.85 for IIDG1, PF 2 = 0.56 for IIDG2, and PF 3 = 0.20 for IIDG3

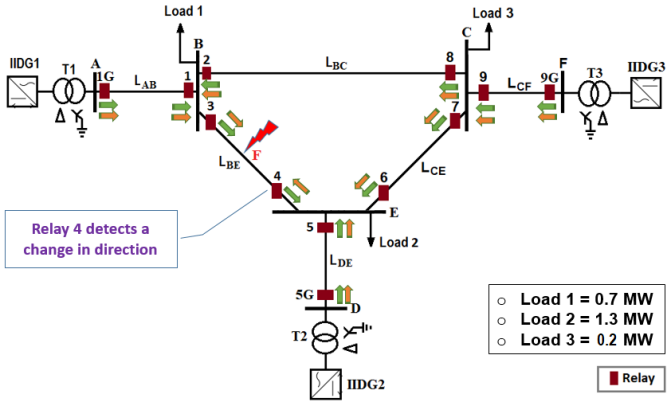


Fig. 7. The illustration of current flow direction through the lines before and after a three-phase fault on Line $L_{BE}$

provided in Table III. The results demonstrate the effectiveness of the proposed protection scheme for all simulated scenarios.

From the table, the first case ($R_f = 0\,\Omega$) under the Reference scenario shows that the scheme is effective for all types of fault. For any type of fault on line $L_{BE}$, consistency in results is observed whereby only Relay 4 registers a change in the cosine value sign (the angle changing from -159.4° to a value of 4th quadrant) as marked in red. With Relay 3 registering no change in cosine value sign, a fault is detected on the line protected by relay pair (3,4). Each of the other relay pairs, (1G,1), (2,8), (5,5G), (6,7), and (9,9G), registers the same transition states, which indicates that there is no fault on their lines. Furthermore, the same consistency in results is obtained for the cases of faults with large range of resistance. For example, Fig. 8 shows that simulation results of a solid

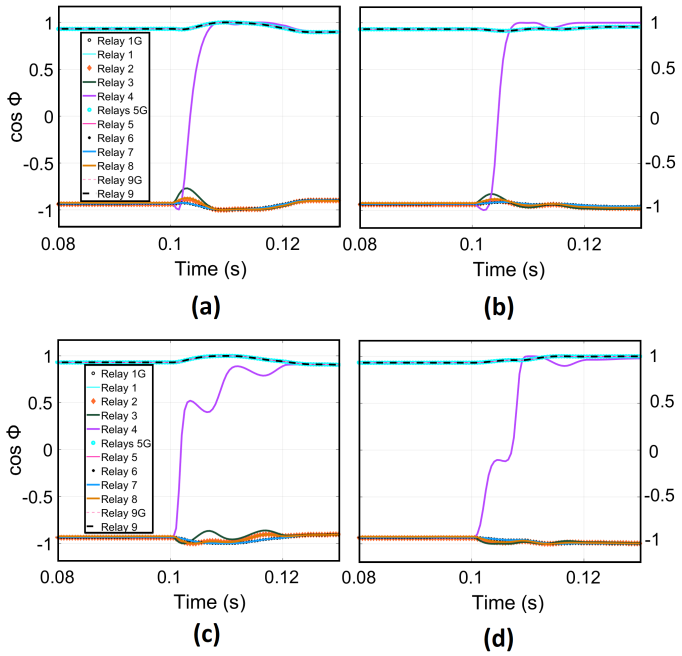


Fig. 8. The cosine values computed by relays with a fault on Line $L_{BE}$: (a) solid line to ground fault (b) line to ground fault with a fault resistance of 100 Ω (c) solid line to line fault (d) line to line fault with a fault resistance of 100 Ω

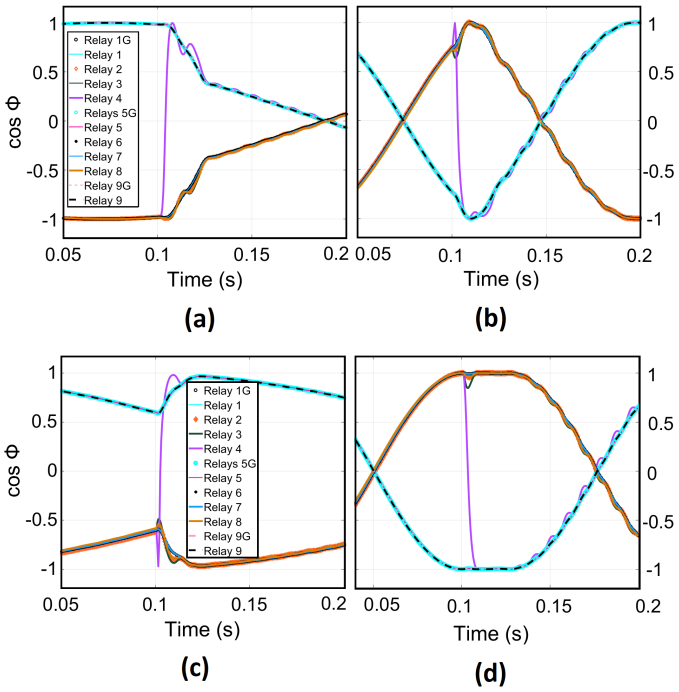


Fig. 9. The cosine values computed by relays with a line to ground fault on Line $L_{BE}$ at $t = 0.1\,s$ with: (a) IIDGs frequency of 49 Hz (b) IIDGs frequency 45 Hz (c) IIDGs frequency of 51 Hz (d) IIDGs frequency 55 Hz

line to ground fault and the same type of fault with a fault resistance of 100 Ω are consistently the same.

The results registered under all the cases of Scenario 1 are also as consistent as those in Reference case. The consistency is clearly obtained for different fault inception time instants, when IIDGs have the same fault currents references as well as when they have different fault current references (i.e. different power factors) as shown in the table.

The results on the discrimination of faults from load switching events are presented in the lower part of the table. In the previous scenarios, results clearly show the effectiveness of the proposed protection approach in detecting faults when the current flows in the faulted line prior to the fault occurrence. The discrimination of fault from load switching event in the previous scenarios is straight-forward as any change in current direction due to load switching event is seen by both relays protecting the line. This is clearly demonstrated with both Relays 3 and 4 registering the change. However, when there is no current flowing in the faulted line prior to fault occurrence depending on the system loading, as explained in Section III.A, the relay pair monitoring directions should be the same to discriminate a fault from load switching.

The state of the system prior to fault or load switching event, as provided in the lower part of Table III, shows that there is no current flowing in Lines $L_{BE}$ and $L_{BC}$ due to initial system loading. When the load is switched into the system at Bus B at the time instant $t = 0.1\ s$, the cosine values computed by Relays 2, 8, 6, and 7 change the sign. However, as they are in pairs i.e (2,8) and (6,7), there is no fault detected. The same situation happens when the load is later disconnected from the system. On the other hand, when a three-phase fault occurs on Line $L_{BE}$, Relay 3 registers a change as well. This clearly indicates a fault on the as the remote relay sees no change.

The slight difference obtained in the angle values throughout the simulation results from relay pairs is not an issue as the sign of the cosine value is rather consistent. This shows that the proposed scheme does not require high precision in the phasor estimates to perform effectively. Furthermore, due to the two-end event comparison approach, erroneous phasor estimates that may be caused by IIDGs generating off-nominal frequencies or unbalanced fault contribution during unsymmetrical faults do not affect the effectiveness of the scheme. This is because the line relay pair experience almost the same effects from the frequency deviation or unbalance. This is shown in Fig. 9 presenting the results from the simulation of a line to ground fault on Line $L_{BE}$ with a wide range of off-nominal frequency (45 Hz, 49 Hz, 51 Hz, and 55 Hz) of IIDGs. From the figure, it is clear that when the fault occurs, Relay 4 registers a change contrary to its counterpart (Relay 3) in all cases. Other than the frequency, other simulation parameters are the same as the ones in reference scenario.

## VI. Conclusions

In order to protect inverter-based microgrids, relays that can overcome challenges brought by unconventional fault signatures of IIDERs are required. These signatures are due to limited and controlled inverter fault currents and it has been acknowledged that differential relays can overcome their challenges among other transmission system- and distribution

system-based protection schemes. However, although technically appropriate, differential relays are not economically viable due to their significantly high communication costs. The proposed microgrid protection relay was derived from an analysis of inverter-based microgrids behavior and allows the use of a low-cost communication system. Its performance demonstrates the effectiveness in all fault conditions and immunity to the inverter fault signatures effect as verified by simulations on the microgrid study system. The analysis in this paper has shown that the proposed scheme offers an advantage of using a low-cost communication system as it requires a low communication bandwidth system. Moreover, the scheme offers inherent immunity to harmonics and noise generated by power electronics, non linear loads, switching transients, and errors in measurements.

## REFERENCES


[1] "Microgrid Protection Systems," Working Group C30, Subcommittee C of the Power System Relaying and Control Committee, July 2019.

[2] J. Shiles et al., "Microgrid protection: An overview of protection strategies in North American microgrid projects," *2017 IEEE Power Energy Society General Meeting*, Chicago, IL, 2017, pp. 1-5.

[3] S. M. Brahma, J. Trejo, and J. Stamp, "Insight into microgrid protection," in *IEEE PES Innovative Smart Grid Technologies Europe,* Istanbul, 2014, pp. 1-6.

[4] CIGRE JWG B5/C6.26/CIRED, "Protection of Distribution Systems with Distributed Energy Resources," 2015.

[5] A. Hooshyar and R. Iravani, "Microgrid protection," in *Proceedings of the IEEE*, vol. 105, no. 7, pp. 13321353, Jul. 2017.

[6] E. Sortomme, J. Ren, and S. S. Venkata, "A differential zone protection scheme for microgrids," *2013 IEEE Power Energy Society General Meeting*, Vancouver, BC, 2013, pp. 1-5.

[7] X. Liu, M. Shahidehpour, Z. Li, X. Liu, Y. Cao and W. Tian, "Protection Scheme for Loop-Based Microgrids," in *IEEE Transactions on Smart Grid,* vol. 8, no. 3, pp. 1340-1349, May 2017.

[8] S. Kar, S. R. Samantaray, and M. D. Zadeh, "Data-Mining Model Based Intelligent Differential Microgrid Protection Scheme," in *IEEE Systems Journal,* vol. 11, no. 2, pp. 1161-1169, June 2017.

[9] S. Chen, N. Tai, C. Fan, C. Fan, J. Liu, and S. Hong, "Sequence-component-based current differential protection for transmission lines connected with IIGs," in *IET Generation, Transmission Distribution,* vol. 12, no. 12, pp. 3086-3096, 10 7 2018.

[10] E. Casagrande, W. L. Woon, H. H. Zeineldin, and D. Svetinovic, "A Differential Sequence Component Protection Scheme for Microgrids With Inverter-Based Distributed Generators," in *IEEE Transactions on Smart Grid,* vol. 5, no. 1, pp. 2937, Jan. 2014.

[11] H. H. Zeineldin, N. H. Kanan, E. Casagrande, and W. L. Woon, "Data mining approach to fault detection for isolated inverter-based microgrids," in *IET Generation, Transmission Distribution,* vol. 7, no. 7, pp. 745-754, July 2013.

[12] M. Xu, G. Zou, C. Xu, W. Sun, and S. Mu, "Positive sequence differential impedance protection for distribution network with IBDGs," *2016 IEEE International Conference on Power System Technology (POWERCON),* Wollongong, NSW, 2016, pp. 1-5.

[13] A. K. Pradhan, A. Routray, and S. Madhan Gudipalli, "Fault Direction Estimation in Radial Distribution System Using Phase Change in Sequence Current," in *IEEE Transactions on Power Delivery,* vol. 22, no. 4, pp. 2065-2071, Oct. 2007.

[14] W. Li, J. He, D. Zhang, and Q. Zhang, "Directional pilot protection based on fault current for distribution network with Distributed Generation (DG)," in *The Journal of Engineering,* vol. 2017, no. 13, pp. 1327-1331, 2017.

[15] H. Gao, J. Li, and B. Xu, "Principle and Implementation of Current Differential Protection in Distribution Networks With High Penetration of DGs," in *IEEE Transactions on Power Delivery,* vol. 32, no. 1, pp. 565-574, Feb. 2017.

[16] J. Yang, C. Zhou, and G. Zou, "A Protection Scheme Based on Positive Sequence Fault Component for Active Distribution Networks," *2018 2nd IEEE Conference on Energy Internet and Energy System Integration (EI2)*, Beijing, 2018, pp. 1-5.

[17] S. Parhizi, H. Lotfi, A. Khodaei and S. Bahramirad, "State of the Art in Research on Microgrids: A Review," in *IEEE Access,* vol. 3, pp. 890-925, 2015.

[18] H.R. Baghaee, M. Mirsalim, G.B. Gharehpetian, H.A. Talebi, "A new current limiting strategy and fault model to improve fault ride-through capability of inverter interfaced DERs in autonomous microgrids", *Sustainable Energy Technology Assessment,* Feb. 2017.

[19] A. H. Kasem Alaboudy, H. H. Zeineldin, and J. Kirtley, "Microgrid stability characterization subsequent to fault-triggered islanding incidents," in *IEEE Transactions on Power Delivery,*, vol. 27, no. 2, pp. 658669, 2012.

[20] A. Ukil, B. Deck, and V. H. Shah, "Current-Only Directional Overcurrent Relay," in *IEEE Sensors Journal,* vol. 11, no. 6, pp. 1403-1404, June 2011.

[21] "Fault Direction Parameter Indicator Device And Related Methods," by A. Ukil, B. Deck, and V. H. SHAH (2016, June 14). Patent US 9,366,715 B2.

[22] C. Zhou, G. Zou, J. Yang and X. Lu, "Principle of Pilot Protection based on Positive Sequence Fault Component in Distribution Networks with Inverter-interfaced Distributed Generators," *2019 IEEE PES GTD Grand International Conference and Exposition Asia (GTD Asia)*, Bangkok, Thailand, 2019, pp. 998-1003.

[23] Q. Li, H. Gao, D. Yu, and B. Xu, "Analysis and verification of a novel current comparison pilot protection," *2017 IEEE Conference on Energy Internet and Energy System Integration (EI2)*, Beijing, 2017, pp. 1-5.

[24] A. G. Phadke, and J. S. Thorp, "Synchronized Phasor Measurements and Their Applications", *Springer Science & Business Media, LLC*, 2008.

[25] S. V Achanta, B. Macleod, E. Sagen, H. Loehner, and S. E. Laboratories, "Apply Radios to Improve the Operation of Electrical Protection," *SEL J. Reliab. Power,* vol. 1, no. 2, pp. 112, 2010.

[26] E. O. Schweitzer, D. Finney, and M. V. Mynam, "Applying radio communication in distribution generation teleprotection schemes," in *2012 65th Annual Conference for Protective Relay Engineers*, 2012, pp. 310320.

[27] "Using Spread Spectrum Radio Communication for Power System Protection Relaying Applications," *IEEE PES PSRC Working Group H2 to the Power System Relaying Committee*, 2005.

[28] MEF, "Microwave Technologies for Carrier Ethernet Services," 2011.

[29] I. E. O. Schweitzer, K. Behrendt, and T. Lee, "Digital Communications for Power System Protection: Security , Availability , and Speed," *SEL J. Reliab. Power,* vol. 1, no. 1, 2010.

[30] D. P. Dickinson, "So Many Wireless Technologies Which Is the Right One for My Application?," 2015.

[31] Vernon Goler, "Using the Universal Asynchronous Receiver Transmitter ( UART ) eTPU Function," 2004.

[32] A. H. K. Alaboudy and H. H. Zeineldin, "Critical clearing time for isolating microgrids with inverter and synchronous based Distributed Generation," in *IEEE PES General Meeting*, 2010, pp. 16.

[33] B. S. I. S. Publication, "Short-circuit currents in three-phase a. c. systems Part 0: Calculation of currents," 2016, p. BS EN 60909-0:2016.